Efficient solid-phase synthesis of meningococcal capsular oligosaccharides enables simple and fast chemoenzymatic vaccine production

Received for publication, October 17, 2017, and in revised form, November 28, 2017 Published, Papers in Press, November 29, 2017, DOI 10.1074/jbc.RA117.000488

Timm Fiebig, Christa Litschko, Friedrich Freiberger, Andrea Bethe, Monika Berger, and Rita Gerardy-Schahn[1]

From the Institute of Clinical Biochemistry, Hannover Medical School, 30625 Hannover, Germany

Edited by Gerald W. Hart

Neisseria meningitidis **serogroups A and X are among the leading causes of bacterial meningitis in the African meningitis belt. Glycoconjugate vaccines, consisting of an antigenic carrier protein coupled to the capsular polysaccharide of the bacterial pathogen, are the most effective strategy for prevention of meningococcal disease. However, the distribution of effective glycoconjugate vaccines in this region is limited by the high cost of cultivating pathogens and purification of their capsular polysaccharides. Moreover, chemical approaches to synthesize oligosaccharide antigens have proven challenging. In the current study, we present a chemoenzymatic approach for generating tailored oligosaccharide fractions ready for activation and coupling to the carrier protein. In a first step, the elongation modes of recombinant capsular polymerases from *Neisseria meningitidis* serogroups A (CsaB) and X (CsxA) were characterized. We observed that CsaB is a distributive enzyme, and CsxA is a processive enzyme. Sequence comparison of these two *stealth* family proteins revealed a C-terminal extension in CsxA, which conferred processivity because of the existence of a second product-binding site. Deletion of the C-terminal domain converted CsxA into a distributive enzyme, allowing facile control of product length by adjusting the ratio of donor to acceptor sugars. Solid-phase fixation of the engineered capsular polymerases enabled rapid production of capsular polysaccharides with high yield and purity. In summary, the tools developed here provide critical steps toward reducing the cost of conjugate vaccine production, which will increase access in regions with the greatest need. Our work also facilitates efforts to study the relationship between oligosaccharide size and antigenicity.**

The prevention of disease and death through vaccination is commonly regarded as one of the major public health achievements of the 20th century and necessary to improve conditions for economic development, particularly in low-income countries (1–3). Historically developed to protect against bacterial pathogens, glycoconjugate vaccines (*i.e.* protein carriers with covalently attached pathogen-specific carbohydrates (4)) are attracting growing attention also as vaccines against protozoa, helminths, viruses, fungi, and even cancer cells (for review see Ref. 5). Indeed, glycoconjugate vaccines are the gold standard to protect against infections caused by encapsulated bacteria like *Haemophilus influenzae* type b, *Streptococcus pneumoniae*, and *Neisseria meningitidis* (4). However, the high complexity and cost of glycoconjugate vaccine production is a barrier to achieving the high vaccination coverage necessary to install herd immunity (3, 6–8). A major obstacle in the production process is the isolation of capsular polysaccharides (CPSs)[2] from large-scale fermentation of bacterial pathogens. This not only is a considerable biohazard but also presents challenges with respect to batch-to-batch reproducibility and a complex downstream purification (8, 9).

Consequently, research in the private sector and academia has focused on developing alternative vaccine production procedures with the aim to completely omit pathogen culture (8, 10–16). A breakthrough in this regard has been the successful marketing of a chemically synthesized *H. influenzae* type b vaccine (15). However, the pure synthetic chemistry approach has not been readily translated to other bacterial pathogens (8).

For several years we have focused our research efforts on establishing safe and effective protocols for the synthesis of urgently needed vaccines. To that end, we exploit the recombinant capsule polymerases (CPs), the key enzymes of CPS synthesis (16–23). In a proof-of-concept study (16), a fully synthetic *Nm*X vaccine has been demonstrated to induce protective antibodies similar to the benchmark vaccine (24). In this study, we develop a streamlined protocol, avoiding steps that present a biohazard and simplifying downstream processing. With the recombinant capsule polymerases from *Nm*X (CsxA) and *Nm*A (CsaB), we describe here a protocol for the tailored synthesis of oligosaccharides of uniform size (avDP15, average degree of polymerization 15) ready for activation and coupling with the carrier protein. Crucial to this procedure was the use of optimized enzymes that enabled solid-phase coupling and control of product length.

This work was supported by LOM (impact-oriented funding) funds to the Institute of Clinical Biochemistry from Medizinische Hochschule Hannover (Hannover Medical School). T. F., M. B., A. B., F. F., and R. G.-S. have submitted patent applications for glycoconjugate vaccines against *Nm*A and *Nm*X.

[1] To whom correspondence should be addressed: Prof. Dr. Rita Gerardy-Schahn, Hannover Medical School, Carl-Neuberg Str. 1, 30625 Hannover, Germany. Tel.: 49-511-532-9802; Fax: 49-511-532-8801; E-mail: gerardy-schahn.rita@mh-hannover.de.

[2] The abbreviations used are: CPS, capsular polysaccharide; avDP, averaged DP; AEC, anion-exchange chromatography; CP, capsule polymerase; CPSA, CPS of *Nm*A; CPSX, CPS of *Nm*X; CsaA, UDP-GlcNAc-2-epimerase; CsaB, capsule polymerase of *N. meningitidis* serogroup A; CsaC, *O*-acetyltransferase; DP, degree of polymerization; MBP, maltose-binding protein; *Nm*A, *N. meningitidis* serogroup A; *Nm*X, *N. meningitidis* serogroup X; primCPS, priming oligosaccharides; SEC, size-exclusion chromatography.

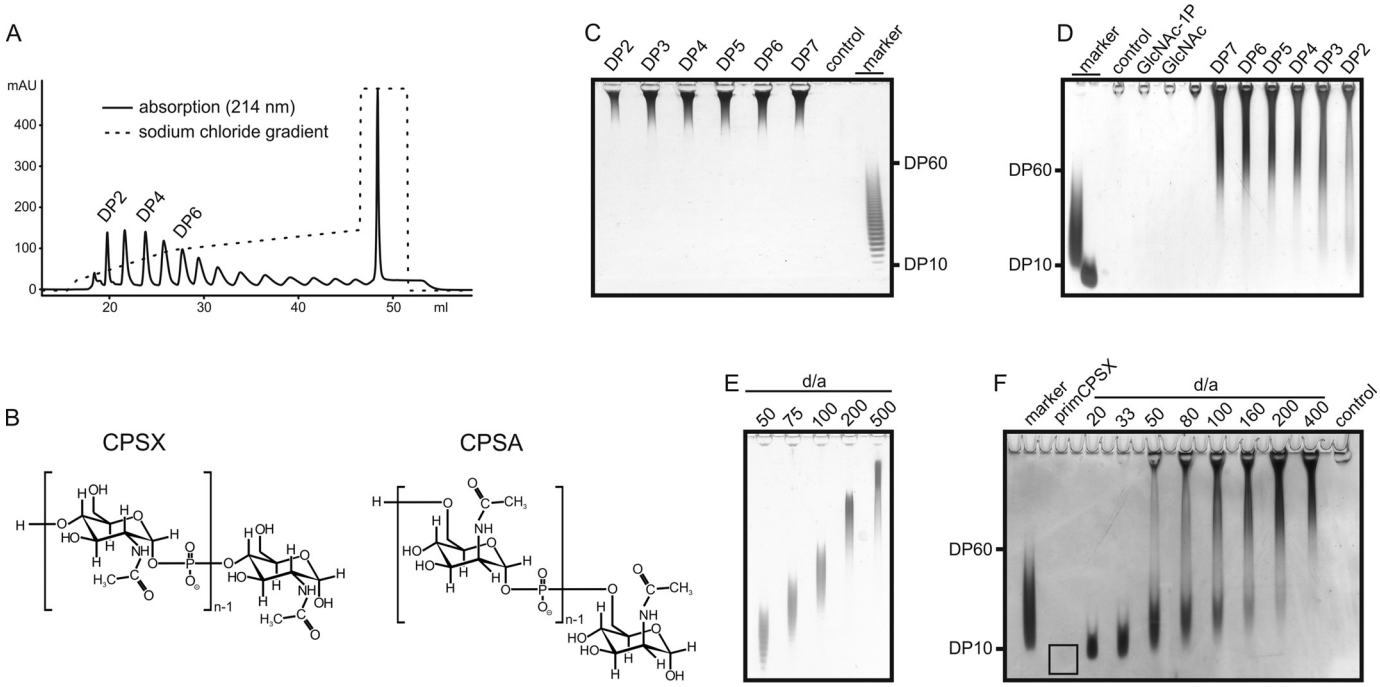

Figure 1. Analysis of the minimal acceptor length and product profiles of CsaB and CsxA. *A*, priming oligosaccharides of defined DP (DP2–DP7) were isolated using AEC. *B*, chemical structures of CPSX and CPSA. *C* and *D*, Alcian blue/silver-stained PAGEs illustrating synthesis products of CsaB (*C*) and CsxA (*D*) reactions in the presence (DP2–DP7) and absence (*control*) of priming oligosaccharides. An oligosaccharide mix (marker, DP10–DP60, avDP15) allows an estimate of the size of the generated CPS. *E*, CsaB reactions performed overnight in the presence of 2 mM donor substrate and varying concentrations of primCPSA demonstrated that the chains produced by CsaB depend on the *d*/*a* ratio. *F*, products of CsxA assembled at varying *d*/*a* ratios were non-uniform. primCPSX loaded onto the gel at the highest concentration used in the assay were not visible (the *black square* marks the position), affirming that all visible products were generated by the enzyme.

Results

Product profiles of recombinant CsxA and CsaB

Oligosaccharides have been shown to induce immune responses superior to long polysaccharides (25). Accordingly, an oligosaccharide fraction comprising DP10–DP60 (see Fig. 1, *C* and *D*, *marker*) is routinely used in glycoconjugate vaccines and prepared from long CPS in two consecutive steps: 1) acidic hydrolysis and 2) sizing (16, 24, 26). With the aim to omit these steps and exploit the enzymatic *in vitro* synthesis to immediately provide oligosaccharides of the required size (avDP15), enzymes that allow direct and facile control of product length are necessary.

The primary feature determining the product-length distribution of CPs is the extent of their interaction with the growing polysaccharide chain (17, 27). Processive enzymes catalyze multiple transfers without intermediate dissociation of the enzyme–product complex (17, 28, 29). Their products are non-uniform. In contrast, enzymes with distributive elongation mode dissociate after each transfer and thus synthesize uniform oligosaccharides ideally of Poisson distribution (17, 30). Under *in vitro* conditions, product-length control can be imposed by the donor to acceptor ratio (*d*/*a*) (17, 30). To obtain insight into the elongation mechanisms of CsaB and CsxA, we used the previously described fusion constructs ΔN69-CsaB$_{co}$-His$_6$ (22) and MBP-CsxA-His$_6$ (21) (for simplicity these constructs are henceforth referred to as CsaB and CsxA).

Assuming that a length bias may be introduced by priming acceptors of varying length, we first tested the polymerases with primers of single DP (DP2–DP7), generated through acid hydrolysis of long CPS and subsequent separation by anion-exchange chromatography (AEC) (Fig. 1, *A* and *B*). Polymerase reactions were performed overnight with catalytic amounts of enzymes (50 nM) and an excess (2 and 5 mM for CsaB and CsxA, respectively) of the donor sugar UDP-GlcNAc (testing of CsaB was carried out in the presence of the epimerase CsaA, needed to produce UDP-ManNAc from UDP-GlcNAc (22)). To visualize products, we used Alcian blue/silver-stained PAGE (Fig. 1, *C* and *D*). Although no (Fig. 1*C*) or only negligible amounts of polymer (Fig. 1*D*) were produced in the absence of primers or presence of free GlcNAc or GlcNAc-1P (Fig. 1*D*), each priming DP (DP2–DP7) was efficiently elongated. Based on these results we decided to use mixtures comprising DP2–DP7 of the respective CPS (henceforth referred to as primCPSA and primCPSX) in experiments aimed to determine the elongation modes of CsxA and CsaB.

In overnight reactions, the polymerases were incubated with priming acceptor (*a*) and donor sugar (*d*; UDP-GlcNAc) in increasing ratios (*d*/*a* ratio). Products were analyzed by Alcian blue/silver-stained PAGE (Fig. 1, *E* and *F*). Unexpectedly, products catalyzed by ΔN69-CsaB$_{co}$-His$_6$ grew in size with the increasing *d*/*a* ratio, indicating a distributive mode of elongation (Fig. 1*E*). In stark contrast, products of CsxA catalyzed reactions were highly dispersed, displaying the typical product profile observed with processive enzymes (Fig. 1*F*).

C-terminal truncation converts CsxA into an enzyme with distributive elongation mode

Both CsaB and CsxA are members of the so called *stealth* protein family, which comprises a number of bacterial virulence factors (31). Characteristic for *stealth* proteins (all are

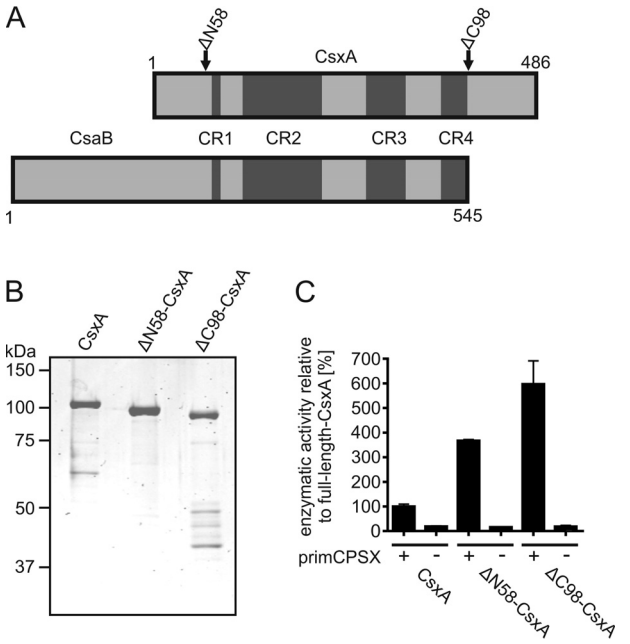

Figure 2. Generation and characterization of CsxA truncation constructs. *A*, CsxA and CsaB were aligned according to their conserved *stealth* protein family regions (CR1–CR4). The first and last amino acid, as well as the sites of truncation introduced into the CsxA sequence, are indicated. *B*, Coomassie-stained SDS-PAGE presenting the purified CsxA constructs. *C*, activity of the purified CsxA constructs in the absence (−) and presence (+) of primCPSX as determined by use of a spectrophotometric assay. Wild-type activity was set to 100%.

hexose-1-phosphate transferases) are four conserved regions (CR1–CR4; Fig. 2*A*). Alignment of the primary sequences of CsaB and CsxA revealed a C-terminal extension of 98 amino acids in CsxA. We hypothesized that this C-terminal extension may confer processivity to the enzyme. To test this hypothesis, the truncation mutant ΔC98-CsxA was constructed. Moreover, because the N-terminal segment preceding CR1 did not show any similarity to the respective domain in CsaB, the mutant ΔN58-CsxA was additionally made. When expressed as recombinant proteins, both truncations were soluble and could be purified via the His_6 tag (Fig. 2*B*) at levels equal to (ΔC98-CsxA, 13 mg/liter culture) or significantly higher (ΔN58-CsxB, 70 mg/liter culture) than wild type. Polymerase activity was tested using a quantifiable spectrophotometric assay (22) with primCPSX as acceptor (Fig. 2*C*). Quite unexpectedly, both truncations showed drastically increased activity (~4-fold ΔN58-CsxA and ~6-fold ΔC98-CsxA).

To test whether the truncations influenced the elongation mode used by CsxA, the assay described in Fig. 1*F* was repeated with the two truncated constructs, by increasing the *d*/*a* ratio stepwise from 20 to 400. After overnight reaction, the products were separated by gel electrophoresis and stained by Alcian blue/silver (Fig. 3, *A* and *B*). The release of the C-terminal 98 amino acids (ΔC98-CsxA) was shown to be sufficient to transform CsxA into a distributive enzyme (Fig. 3*A*). In contrast, truncation of the N-terminal 58 amino acids had no considerable impact on the elongation mode (Fig. 3*B*). To confirm these data, we additionally monitored the product profiles of CsxA truncations in a time-course experiment. As an analytical system, we used HPLC-based AEC (22). To exclude any bias at acceptor site, the time-course experiment was carried out with DP5 as priming substrate. After reaction start (time point 0′), samples were taken as indicated (Fig. 3, *C* and *D*). In perfect agreement with the PAGE results (Fig. 3*B*), ΔN58-CsxA synthesized short oligosaccharides in the early reaction phase (Fig. 3*D*). After 20 min, a second well-separated peak representing long polysaccharides appeared. Because chains of DP > 18 were only present in minor quantities, this profile allowed to conclude that chains of DP > 18 are necessary to start processive elongation. Conversely, the products of ΔC98-CsxA were observed to grow continuously throughout the reaction, confirming the distributive mode of elongation of this enzyme (Fig. 3*C*).

Two models exist in the literature on the basis of which the prominence of the C terminus for CsxA processivity could be explained: 1) Similar to enzymes acting on DNA (*e.g.* helicases; reviewed in Ref. 29), the C terminus might assist in the formation of an oligomeric structure that encloses the nascent chain as soon as an intermediate chain length is reached (Fig. 4*A*); and 2) in analogy to other enzymes producing carbohydrate polymers, the C terminus might harbor an extended binding site with increasing affinity for the growing polymer chain (Fig. 4*B*) (17, 27). Because we knew from earlier work that wild-type CsxA elutes as an oligomer (depending on the salt concentration with an apparent molecular mass of an octamer or tritetramer) from size-exclusion chromatography (SEC) columns (21), we first asked whether depletion of the C terminus altered the oligomerization state. As shown in Fig. 4, ΔC98-CsxA, similar to the wild type, migrated as an octamer in low salt buffer (Fig. 4*C*) and formed assemblies >trimer in high salt buffer (Fig. 4*D*). Rather unexpectedly, the processive ΔN58-CsxA, used as a control in these experiments, eluted as a dimer in both high and low salt buffer (Fig. 4, *C* and *D*). These data revealed that the N terminus determines the oligomeric state of CsxA and in addition showed that processivity in CsxA is independent of the oligomeric state. Consequently, we evaluated the second possibility, the existence of a second product-binding site in the C-terminal domain. For this purpose, the construct ΔN387-CsxA-His_6, which comprises only the C-terminal 99 amino acids, was cloned and expressed. As a simple binding assay, we studied the sensitivity of the purified protein against proteinase K in the presence and absence of CPSX. The Coomassie-stained SDS-PAGE used to monitor the time-dependent proteolysis is shown in Fig. 4*E*. In the presence of CPSX, proteolytic degradation of the C-terminal domain was significantly delayed. Although compared with the starting material, a size reduction became visible shortly after proteinase K contact (5 min), this first degradation product remained visible for 300 min when CPSX was present. In the absence of CPSX as well as in the presence of CPSA (Fig. 4*F*), this band was drastically reduced already after 30 min and completely disappeared after 90 min. Together, these results provide strong arguments for a specific binding of CPSX to the C-terminal domain and thus for the existence of a second product-binding site in CsxA.

Finally, we asked whether also the double truncated CsxA can be produced and cloned the mutant ΔN58ΔC98-CsxA. If compared with CsxA and ΔC98-CsxA, ΔN58ΔC98-CsxA could be purified to homogeneity, almost completely lacking degra-

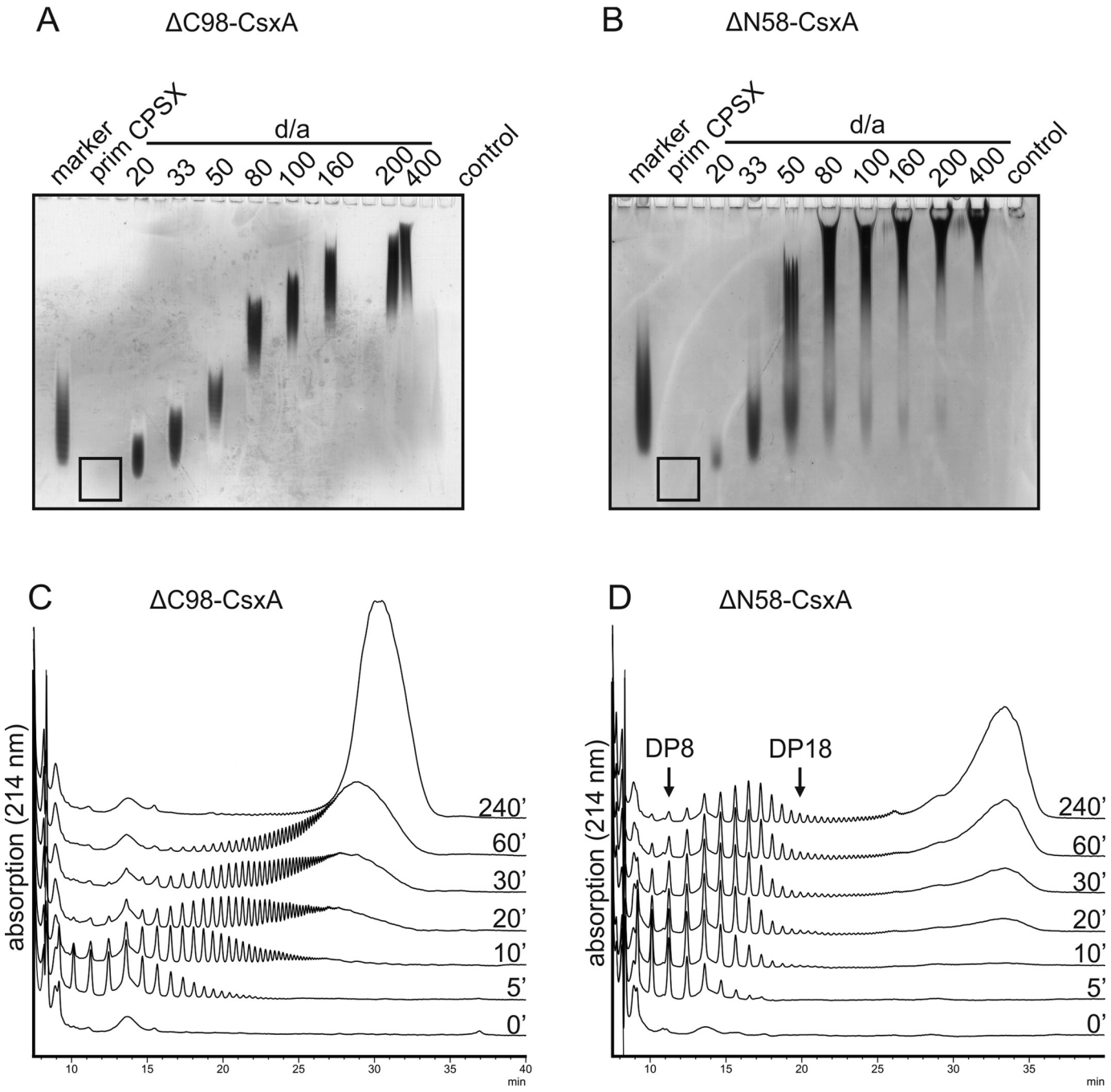

Figure 3. Product profiles of CsxA truncations. *A* and *B*, products generated by ΔC98-CsxA (*A*) and ΔN58-CsxA (*B*) at increasing *d*/*a* ratios after overnight incubation. Oligosaccharide fractions of avDP15 were loaded as marker. The *squares* indicate the gel positions of primCPSs. *C* and *D*, time-course experiments presenting the reaction products catalyzed by ΔC98-CsxA (*C*) and ΔN58-CsxA (*D*). The elongation reactions were primed with DP5, and samples were taken at indicated time points. Products were resolved by HPLC-AEC. Previous calibration of the column with individual DPs allowed the assignment of single peaks.

dation products (compare Fig. 2*B* and Fig. 5*A*). The purification yield (27 mg/liter culture) was intermediate between ΔN58-CsxA (70 mg/liter culture) and ΔC98-CsxA (13 mg/liter culture). In SEC, the construct appeared to be mono- to dimeric, independent of the salt concentration (Fig. 5, *B* and *C*). The product profile produced at a *d*/*a* ratio of 20 was even narrower than the one produced by ΔC98-CsxA (Fig. 5*D*) and more closely resembled the dispersity of the fraction used for vaccine production (marker). Finally, a time-course experiment was conducted to examine the elongation mode of the double truncated enzyme. With DP5 as a primer, ΔN58ΔC98-CsxA generated a narrow Poissonian product distribution at all sampled time points (Fig. 5*E*). Taken together, this protein perfectly suited the requirements of vaccine production.

On-column synthesis of length controlled CPSX oligosaccharides

Solid-phase fixation of enzymes in biotechnological processes is of major value, because this measure supports protein longevity, reduces the need for protein production because

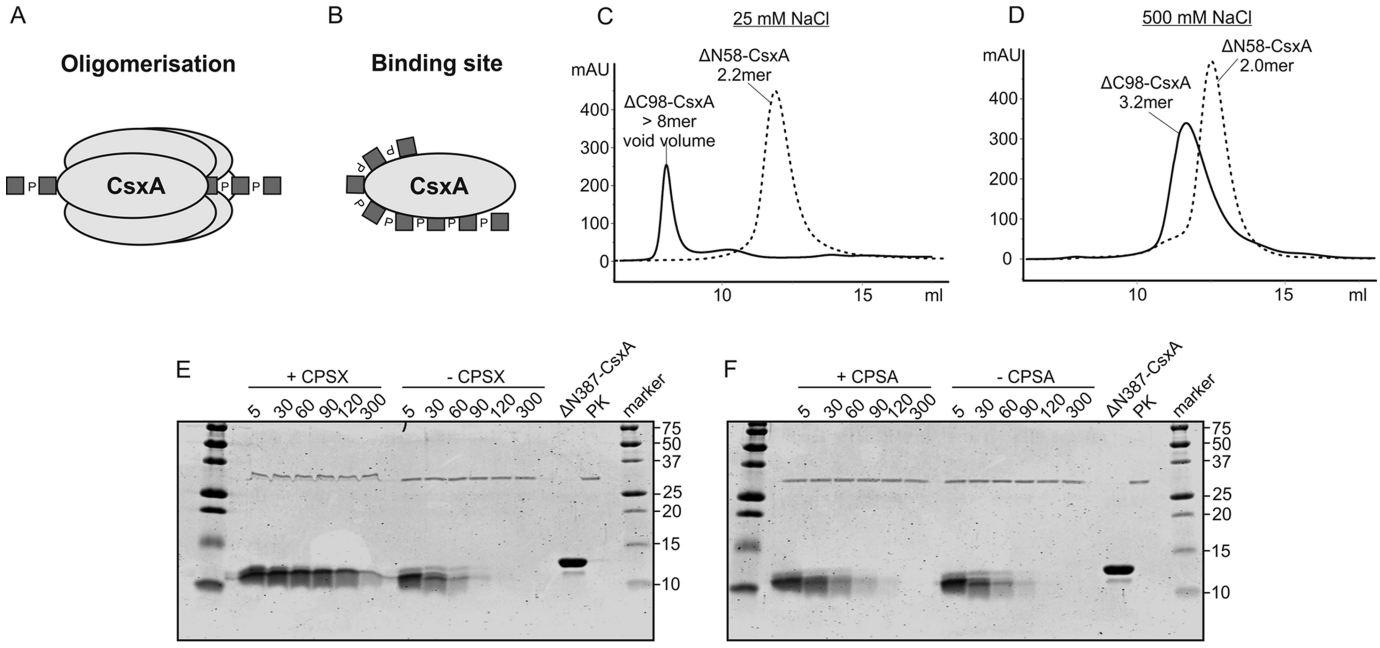

Figure 4. The C terminus of CsxA contains an extended product-binding site. Two models exist in literature that may explain the role of the CsxA C-terminal domain in mediating processivity. *A*, elements in this domain promote the formation of an oligomeric structure that encloses the growing CPS chain. *B*, the C terminus harbors a second CPS binding site. *C* and *D*, in size-exclusion chromatography the oligomeric state of the truncated CsxA constructs was determined under low-salt (*C*) and high-salt (*D*) conditions. Although the C-terminally truncated protein eluted very similar to wild type (21), the protein formed an apparent dimer after removal of the N-terminal 58 amino acids. *E* and *F*, proteinase K sensitivity of the isolated C-terminal domain (ΔN387-CsxA) was assayed in the presence and absence of CPSX (*E*) and CPSA (*F*). The delayed degradation of the protein in the presence of CPSX but not CPSA argues for a specific binding of the first. As control, the purified ΔN387-CsxA and proteinase K (*PK*) were loaded onto the gel.

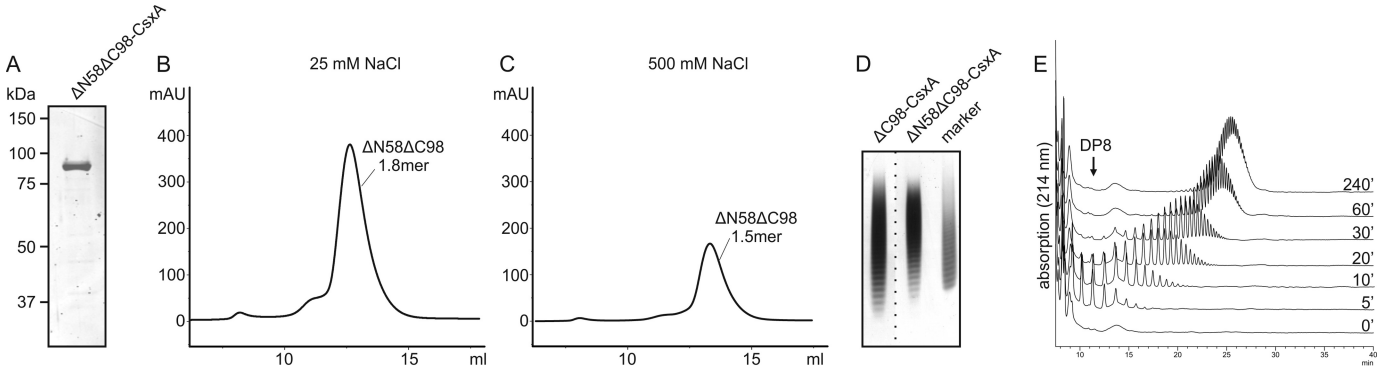

Figure 5. The double truncated protein ΔN58ΔC99-CsxA is distributive with near Poissonian product profile. *A*, Coomassie-stained SDS-PAGE showing purified ΔN58ΔC98-CsxA. *B* and *C*, SEC experiments carried out with ΔN58ΔC98-CsxA under low-salt (*B*) and high-salt (*C*) conditions indicate a mono- to dimeric assembly. *D*, Alcian blue/silver-stained PAGE comparing the products synthesized by ΔC98-CsxA and ΔN58ΔC98-CsxA. The marker was obtained from the vaccine manufacturer GlaxoSmithKline and is identical to the CPSX fraction of avDP15 used in vaccine production protocols. The *dashed line* indicates that samples irrelevant for this figure were excised. *E*, time-course experiment demonstrating reaction products catalyzed by ΔN58ΔC98-CsxA after priming with DP5. The HPLC-AEC profiles indicate a near Poissonian distribution of products over the entire time frame.

enzyme-loaded matrices are reusable, and facilitates downstream processes (32). In a pilot experiment, ΔN58ΔC98-CsxA was loaded onto a HisTrap column (ΔN58ΔC98-CsxA is N-terminally MBP-tagged and C-terminally His-tagged). After extensive washing, a reaction mixture containing primCPSX and UDP-GlcNAc in the ratio 1:20 was continuously pumped through the column with a peristaltic pump (Fig. 6*A*). The reaction progress was monitored every 20 min in an HPLC-based assay that allowed the parallel detection of UDP-GlcNAc and UMP at 280 nm (Fig. 6*B*). After 100 min, only UMP was detected and indicated complete consumption of UDP-GlcNAc. Size and dispersity of oligosaccharides was analyzed by Alcian blue/silver-stained PAGE (Fig. 6*C*) and HPLC-AEC (Fig. 6*D*). Both analyses demonstrated that the product dispersity was identical to the oligosaccharide marker (avDP15), which was obtained by the conventional vaccine production protocols (24) (Fig. 6, *C* and *D*). To ensure that oligosaccharide fractions are not contaminated with enzyme that may bleed off the HisTrap matrix, this column was connected with an amylose column, an affinity matrix for MBP (Fig. 6*A*). The amylose column was eluted after 100 min of production time, but no protein was detected in the eluate (data not shown). Similarly, we were unable to detect the enzyme in the reservoir from which samples were taken every 20 min (Fig. 6*E*). In contrast, when imidazole buffer was added to the HisTrap column at the end of the reaction, a sharp enzyme band identical to purified ΔN58ΔC98-CsxA was visible (compare Figs. 5*A* and 6*E*). Taken together, these experiments for the first time describe a simple,

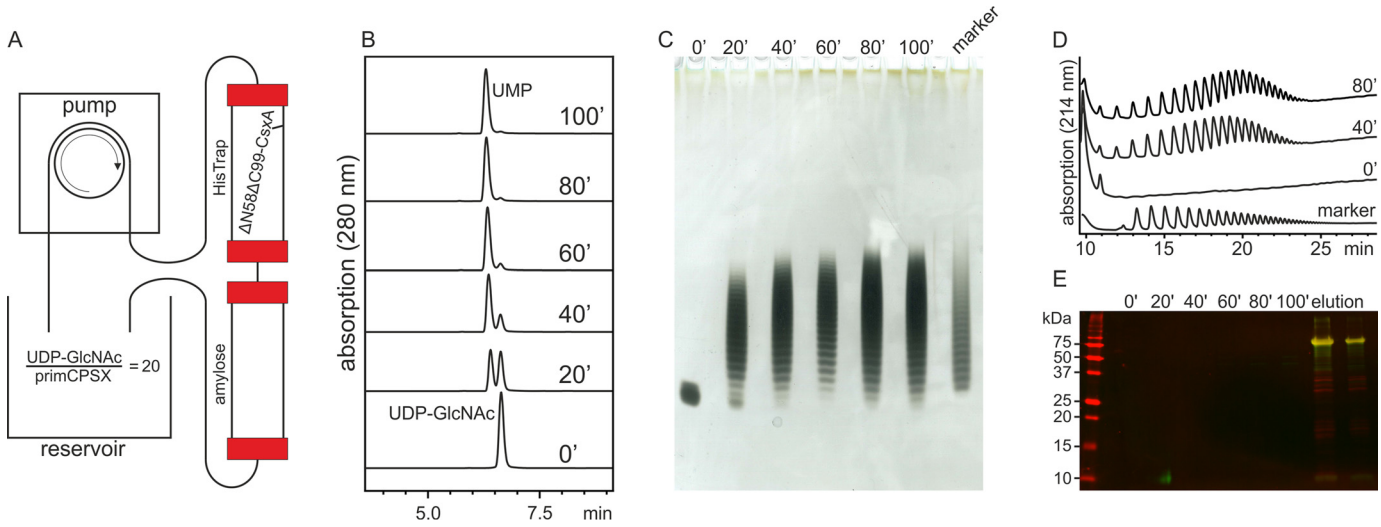

Figure 6. Solid-phase synthesis of CPSX oligosaccharides. *A*, schematic of the experimental setup. A reaction mix containing UDP-GlcNAc and primCPSX was circulated through a HisTrap column containing immobilized ΔN58ΔC98-CsxA, and an amylose column was linked to retain bled-off protein. *B*, UDP-GlcNAc consumption and parallel UMP production were determined by HPLC-AEC to follow the progress of the reaction. *C* and *D*, Alcian blue/silver-stained PAGE (*C*) and HPLC-AEC (*D*) were used to compare the dispersity of the enzymatically generated oligosaccharides to marker material from vaccine manufacturing. *E*, Western blot analysis developed against the N-terminal MBP tag (*green channel*) and the C-terminal His_6 tag (*red channel*) demonstrated that, at all sampled time points, the reaction mixture was free of protein, whereas elution of the HisTrap column with imidazole released the protein.

fast, and efficient protocol for the synthesis of oligosaccharides ready for activation and protein coupling.

Length controlled CPSA oligosaccharides by use of a CsaB–CsaA fusion enzyme

Although CsaB was demonstrated to exhibit a distributive elongation mode (Fig. 1*E*), the on-column synthesis of CPSA is challenging, because the donor sugar UDP-ManNAc is unstable and not commercially available. Thus, in-process production of UDP-ManNAc from UDP-GlcNAc by use of the epimerase CsaA is necessary (22) and was planned in this study. From previous work with the soluble enzymes in a one-pot reaction, we knew that CPSA synthesis was efficient as long as the concentration of CsaB was equal or higher than the concentration of CsaA (22). Therefore, we assumed that the generation of a fusion protein would best comply with the requirements for the on-column synthesis and also reduce efforts with respect to protein purification and downstream processing. Guided by our previous observation that a free N terminus increases CsaB expression levels (22), the construct CsaB–CsaA was cloned with C-terminal His_6 tag and purified at a yield of 30 mg/liter expression culture. To confirm activity, CsaB–CsaA was incubated with primCPSA and UDP-GlcNAc in increasing *d*/*a* ratios (Fig. 7*A*). This test series confirmed that fusion with CsaA did not alter the elongation mode of CsaB.

To obtain proof-of-concept that also CPSA synthesis can be carried out on a solid phase, the fusion protein was loaded onto a HisTrap column as described for CsxA. However, because we had learned in the previous experiment that the reaction slowed down with time because of continuous dilution of substrates in the reservoir (Fig. 6, *A* and *B*), we modified the experimental setup and loaded the entire reaction mixture (10 ml), containing a *d*/*a* ratio of 20, in one step. Samples were taken for HPLC-AEC, PAGE, and Western blot analysis, before the collected fractions (2 ml) were pooled and loaded for a second time. The HPLC-AEC analysis of the first and second load showed that 78 and 89% of UDP-GlcNAc was consumed, respectively (Fig. 7*B*). Product size evaluation was carried out with Alcian blue/silver-stained PAGE and, as in the case of CPSX, demonstrated a dispersity highly similar to the marker material (Fig. 7*C*). As before, we did not see any contamination of the oligosaccharide fractions with protein but could elute the enzyme from HisTrap by adding imidazole buffer (Fig. 7*D*). However, it is of note that a second His_6-tagged band migrating with the theoretical molecular mass of CsaA-His_6 was present in both the soluble lysate and (even enriched) the eluate of the HisTrap column. This second band by all likelihood indicates partial degradation of the fusion protein CsaB–CsaA during expression. Thus, future work will aim to stabilize the fusion protein. This proof-of-concept study clearly highlights the advantage of enzyme catalyzed vaccine production protocols.

Discussion

For the first time, we describe in this study the comprehensive characterization of the elongation mechanisms of two polymerizing *N*-acetylhexosamine-1-phosphate transferases (CsaB and CsxA) of the *stealth* protein family and their use as biotechnological tools for the production of tailored CPS fragments of the meningococcal serogroups A and X. The decision to study these two enzymes was made on the basis that *Nm*A and *Nm*X represent considerable threats to public health (33). Moreover, no licensed vaccine exists for *Nm*X, and, despite the successful introduction of the anti-*Nm*A vaccine MenAfriVac™ (34, 35), stockpiling of vaccines and/or vaccine components as requested by the International Coordinating Group on Vaccine Provision for Epidemic Meningitis is particularly difficult in the case of the short-lived CPSA (7, 36). Last, but certainly not least, current protocols are not suited to promote decentralized production of vaccines to allow immediate responses to unforeseeable needs foremost occurring in developing countries (6, 7).

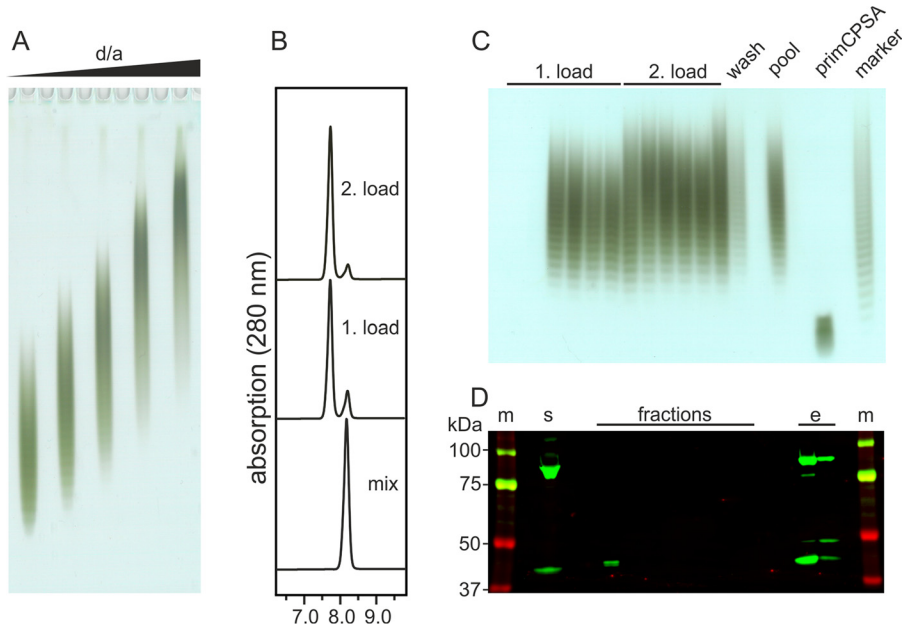

Figure 7. Solid-phase synthesis of CPSA oligosaccharides. *A*, Alcian blue/silver-stained PAGE of CPSA generated in CsaB–CsaA reactions at varying *d*/*a* ratios. *B*, HPLC-AEC chromatograms documenting the reaction progress by detecting UDP-GlcNAc (*right peak*) and UMP (*left peak*) in the reaction mix before loading and in a representative fraction after the first and the second load. *C*, Alcian blue/silver-stained PAGE of all collected fractions for visualization of CPSA. *D*, Western blot analysis demonstrating stable attachment of CsaB–CsaA to the column matrix until elution performed with imidazole. *Lanes m*, marker; *lane s*, soluble fraction of *E. coli* lysate used to prepare the enzyme loaded column; *lane e*, protein eluted with imidazole after the reaction.

Synthetic chemistry promises an alternative source of CPS fragments, which avoids the need for large-scale cultivation of pathogens (8, 11–13, 15, 37). Compared with the use of enzymes, chemical processes require time-intensive multistep procedures to build the complex CPS fragments. With regard to meningococcal vaccines against serogroups A and X, the longest compounds obtained by chemical synthesis are the CPSX and CPSA tetramers (10, 11). Mouse immunization experiments were performed with a protein coupled CPSX trimer (12) and a trimer of a CPSA carba-analogue (13). Although both antigens induced a specific antibody response, it was low compared with the natural polymer with the average DP of 15 used as benchmark (24, 26).

In the current proof-of-concept study, we produced 8 mg of CPSA of avDP15 and 70 mg of CPSX of avDP15 (see "Experimental procedures") in less than 2 h using standard laboratory equipment (*E. coli* safety strain for expression, 1-ml commercial HisTrap columns, simple peristaltic pump) and without any further investment in process optimization. The straightforward protocol and avoidance of biohazard shall facilitate the adaptation to low-tech environments.

Covalent chemical coupling of carbohydrate antigens to protein carriers generates glycoconjugate vaccines that elicit T-cell help for B cells recognizing the carbohydrate epitope and, consequently, isotype switching from IgM to IgG (38). A recent study reported that the carbohydrate component of a group B *Streptococcus* glycoconjugate vaccine is processed by antigen presenting cells to 10 kDa (≈50 hexoses) in size (38, 39). On the other hand, small synthetic oligosaccharides (DP 3–4) have been shown to elicit functional antibody responses, although at a low level, if conjugated to a carrier protein (12, 38). Our technology provides a valuable tool for the generation of tailored oligosaccharide fractions that can be used to investigate the dependences of antigen size and immunogenicity in vaccine development studies.

Large CPS binding sites have been postulated for several CPs from encapsulated bacteria (both Gram-negative and Gram-positive strains). For example, the polysialyltranferase from *Nm*B was shown to accommodate chains of at least 20 residues (17), whereas the extended binding site in the *E. coli* K92 enzyme may bind up to 10–12 residues (40). The CP from *S. pneumoniae* was shown to switch to processive elongation with acceptors greater than an octasaccharide (27). However, none of the enzymes studied to date have been shown to harbor a distinct processivity-conferring polysaccharide binding domain. Of note in this context, a blast search with the C-terminal 98 amino acids of CsxA did not identify any homologous sequences.

Hypothesizing that in ΔN69-CsaB$_{co}$-His$_6$ a processivity mediating element was cut off, we also analyzed reaction products formed by full-length CsaB, but no processive elongation was seen (data not shown). A potential explanation for the distributive elongation mode of CsaB could be that *in vivo* the protein interacts with additional enzymes (*e.g.* the epimerase CsaA and the *O*-acetyltransferase CsaC) (22), which confer processivity. Moreover, distributive chain elongation by CsaB may be required for CsaC to generate uniform *O*-acetylation patterns. Further research is needed to answer these open questions.

When analyzed with the help of bioinformatics tools like globplot (41) and PHYRE2 (42), the N-terminal 58 amino acids of CsxA were predicted to be disordered. Removal as in construct ΔN58-CsxA was therefore expected to improve expression levels and protein stability. Indeed, the observed dispensability of the N terminus of the recombinant CsxA and CsaB

Table 1
Primers used in this study
The restriction sites are highlighted in bold type.

Primer pair	Resulting construct
CG**GGATCC**CCAATTGAAGATCCATACCCAGTA CCG**CTCGAG**TTGTCCACTAGGCTGTGATG	*pMBP-ΔN58-csxA-His*$_6$
GC**GGATCC**ATTATGAGCAAAATTAGCAAATTG CCG**CTCGAG**GAGAATTTCTGCTTCTGATACATC	*pMBP-ΔC98-csxA-His*$_6$[a]
CG**GGATCC**CCAATTGAAGATCCATACCCAGTA CCG**CTCGAG**GAGAATTTCTGCTTCTGATACATC	*pMBP-ΔN58ΔC98-csxA-His*$_6$
GCATCT**CATATG**CTTCCTACTAAATCTGAAG TAGCTG	*pΔN387-csxA*[a]
GCATCT**CTCGAG**TTGTCCACTAGGCTGTGATGTG	
GCATCT**CATATG**CTGATCCCGATCAATTTCTTT GC**GGATCC**GTTATTGTTATTGTTGTTGTTATTG TTATTGGAGCTCGATTTCTCGAAGGAGCTCG GCAACGG	*pΔN69-csaB*$_{co}$*-csaA-His6*
GC**GGATCC**AAAGTCTTAACCGTCTTTGGC CCG**CTCGAG**TCTATTCTTTAATAAAGTTTCTACA	*pΔN69-csaB*$_{co}$*-**csaA**-His6*

[a] Leucine 388 of the CsxA sequence, normally encoded by ctt, is encoded by ctc from the XhoI site used for cloning.

prompts us to speculate that these protein domains fulfill functions that are needed only in the *in vivo* situation (22).

More research is also needed to produce a stable CsaB–CsaA fusion construct and will be carried out in the same way as our previous work with protease-resistant linkers (21, 43). Still, it is noteworthy that the partial breakdown of the fusion protein did not negatively influence the on-column production. Indeed, it is conceivable that higher CsaA concentrations established by column retention of the His_6-tagged protein were of advantage. Generally, there is significant room to further improve the on-column procedure. One important measure for instance would be covalent enzyme coupling to facilitate the reuse of matrices (32).

Considering that chemists can synthesize native CPSA and CPSX fragments containing the necessary chemical functionality for downstream protein coupling (10–12), it is an interesting idea to combine the advantages of the here-described enzyme catalyzed CPS synthesis with chemically optimized primers into a platform that advances the fast and reliable provision of oligosaccharides ready for protein coupling.

Experimental procedures

General cloning

The generation of *pMBP-csxA-His*$_6$ and *pΔ69-csaB*$_{co}$*-His*$_6$ has been reported elsewhere (21, 22). All truncated CsxA constructs described herein were amplified by PCR using the primers shown in Table 1 and plasmid pHC19 described in Ref. 21 as template. After restriction digest using the restriction sites shown in Table 1 (highlighted in bold text), *csxA* truncations were cloned via BamHI/XhoI into *pMBP-csxA-His*$_6$ (*tac*) (21). *pΔN387-csxA-His*$_6$ was generated by replacing *MBP-csxA* in *pMBP-csxA-His*$_6$ (*tac*) with *ΔN387-csxA* (NdeI/XhoI). For the generation of the fusion construct *pΔN69-csaB*$_{co}$*-csaA-His*$_6$, *csxA* in *pMBP-csxA-His*$_6$ (*tac*) was replaced with *csaA* (BamHI/XhoI), and *MBP* was replaced with *ΔN69-csaB*$_{co}$ (NdeI/BamHI).

Expression, purification, and activity testing of recombinant CsaB and CsxA constructs

Expression and purification of all CsaB- and CsxA-based sequences was performed as described in Refs. 22 and 21, respectively. The spectrophotometric assay published for CsaB (22) was adapted for CsxA, resulting in the alterations as follows: 1) no CsaA (epimerase) was used in the reaction mixture, 2) the reaction was performed using 54 nM of the respective CsxA construct in the presence of 3) 37 ng of CPSX oligosaccharides of avDP18.6.

SDS-PAGE and immunoblotting

SDS-PAGE and immunoblotting were performed as described before (21, 22).

Purification of CPSA and CPSX oligosaccharides

The marker, previously described as oligosaccharides of avDP15 (DP10–DP60) (16, 21, 22, 24), was obtained from the vaccine manufacturer GlaxoSmithKline (Siena, Italy). CPSA and CPSX oligosaccharide mixtures (primCPS) (16, 21, 22) were dephosphorylated using either acid phosphatase (Sigma) or calf intestinal alkaline phosphatase (New England Biolabs) according to the manufacturer's guidelines. AEC was performed on an $ÄKTA_{FPLC}$ (GE Healthcare) equipped with a MonoQ HR 5/5 column (GE Healthcare) at a flow rate of 1 ml/min. H_2O and 1 M NaCl were used as mobile phases M_1 and M_2, respectively. Samples were separated using a combination of linear gradients (0–5% over 1 ml, 5–20% over 10 ml, and 20–30% over 20 ml). Acetate and GlcNAc-1P were used to calibrate the column. The amount of oligosaccharide in each fraction was estimated from the peak area obtained at 214 nm under the assumption that each residue contributes equally to the absorbance of the respective oligomer. Fractions were dialyzed against water (ZelluTrans, Roth, 1-kDa molecular mass cutoff) and freeze-dried, and equal concentrations were adjusted with H_2O. The identity and DP of the oligosaccharide fractions was confirmed by HPLC-PAD (pulsed amperometric detection) using established protocols (36).

Analysis of CsaB and CsxA reaction products

For the *d*/*a*-dependent analysis, 100 nM CsaB and 50 nM CsxA constructs were incubated in 25–100 μl of reaction buffer (50 mM Tris, pH 8.0, 20 mM $MgCl_2$ (2 mM DTT, only for CsxA)) in the presence of 2 mM (CsaB) or 5 mM (CsxA) UDP-GlcNAc and acceptors in a concentration resulting in the *d*/*a* ratios indicated in Figs. 1 and 3. CsaB reactions were supplemented with 0.1 μM CsaA for *in situ* UDP-ManNAc production.

For the time-dependent analysis, the reaction volume was up-scaled to 700 μl, the UDP-GlcNAc concentration was increased to 10 mM, and DP5 was used as primer (*d*/*a* ratio of 500). Aliquots were snap-frozen after the indicated time points and heat-inactivated for 3–5 min at 98 °C prior to analysis. HPLC-AEC and high percentage PAGE followed by Alcian blue/silver staining was performed as described before (22).

Analytical size-exclusion chromatography

Roughly 300 μg of recombinant protein was analyzed at 280 nm on an $ÄKTA_{FPLC}$ (GE Healthcare) equipped with a Superdex 10/300 GL column (GE Healthcare) using 50 mM Tris, pH 8.0, as elution buffer supplemented with NaCl as indicated in Fig. 4. For the analysis of CsxA constructs, 1 mM of DTT was added. The column was calibrated using the gel filtration markers kit for protein molecular masses 29,000–700,000 Da (Sigma) according to the manufacturer's guidelines.

Limited proteolysis

Samples containing 22 μg of ΔN387-csxA-His_6, 2.2 μg of proteinase K, and if present, 0.4 mg of CPSX or CPSA in a volume of 100 μl of PBS were incubated at room temperature. Aliquots were taken at the indicated time points, frozen at −20 °C, and analyzed by SDS-PAGE as previously described (21, 22).

Solid-phase synthesis

According to the published purification protocols for CsxA and CsaB (21, 22), ΔN58ΔC98-CsxA and CsaB–CsaA were expressed in M15(pREP4) and BL21(DE3), respectively. 50–100 ml of expression culture were lysed, coupled to a 1-ml HisTrap (GE Healthcare) column and thoroughly washed with 1) binding buffer (50 mM Tris, pH 8.0, 500 mM NaCl, 35 mM imidazole (1 mM DTT only for CsxA constructs)) and 2) equilibration buffer (50 mM Tris, pH 8.0, (1 mM DTT only for CsxA constructs) on an $ÄKTA_{FPLC}$ (GE Healthcare) until a stable base line was established. The HisTrap column was connected to a peristaltic pump P1 (GE Healthcare); 10 ml (for CPSA synthesis) or 19 ml (for CPSX synthesis) of reaction mix (50 mM Tris, pH 8.0, 20 mM $MgCl_2$, UDP-GlcNAc (10 mM for CsxA, 2 mM for CsaB–CsaA reactions), primCPS at a *d*/*a* ratio of 20) was pumped through with a flow-rate of 0.25–0.5 ml/min; and fractions were collected as indicated in Figs. 6 and 7. Samples were analyzed by SDS-PAGE, Alcian blue/silver-stained PAGE, and HPLC-AEC as described above.

Author contributions—T. F. and R. G.-S. conceptualization; T. F. supervision; T. F., C. L., F. F., A. B., and M. B. investigation; T. F. methodology; T. F. and R. G.-S. writing-original draft; C. L. writing-review and editing; R. G.-S. funding acquisition; T. F. and R. G.-S. designed the study and wrote the paper.

Acknowledgments—We thank Dr. Francescso Berti, Dr. Roberto Adamo, Dr. Maria Rosaria Romano, Dr. Daniela Proietti, and Davide Oldrini (all GlaxoSmithKline vaccines) for helpful discussions and technical advice. We thank Dr. Timothy G. Keys (ETH, Zurich, Switzerland) for critically revising the manuscript.

References

1. Centers for Disease Control and Prevention (CDC) (2011) Ten great public health achievements: worldwide, 2001–2010. *MMWR Morb. Mortal. Wkly. Rep.* **60,** 814–818 Medline
2. Bärnighausen, T., Bloom, D. E., Cafiero-Fonseca, E. T., and O'Brien, J. C. (2014) Valuing vaccination. *Proc. Natl. Acad. Sci. U.S.A.* **111,** 12313–12319 CrossRef Medline
3. Levine, O. S., Bloom, D. E., Cherian, T., de Quadros, C., Sow, S., Wecker, J., Duclos, P., and Greenwood, B. (2011) The future of immunisation policy, implementation, and financing. *Lancet* **378,** 439–448
4. Pace, D. (2013) Glycoconjugate vaccines. *Expert Opin. Biol. Ther.* **13,** 11–33 CrossRef Medline
5. Astronomo, R. D., and Burton, D. R. (2010) Carbohydrate vaccines: developing sweet solutions to sticky situations? *Nat. Rev. Drug Discov.* **9,** 308–324 CrossRef Medline
6. Maurice, J. (2015) Vaccine shortage threatens spread of meningitis in Niger. *Lancet* **385,** 2241 CrossRef Medline
7. World Health Organization (2017) Epidemic meningitis control in countries of the African meningitis belt, 2016. *Wkly. Epidemiol. Rec.* **92,** 145–154 Medline
8. Adamo, R. (2017) Advancing homogeneous antimicrobial glycoconjugate vaccines. *Acc. Chem. Res.* **50,** 1270–1279 CrossRef Medline
9. Costantino, P., Rappuoli, R., and Berti, F. (2011) The design of semi-synthetic and synthetic glycoconjugate vaccines. *Expert Opin. Drug Discov.* **6,** 1045–1066 CrossRef Medline
10. Harale, K. R., Rout, J. K., Chhikara, M. K., Gill, D. S., and Misra, A. K. (2017) Synthesis and immunochemical evaluation of a novel *Neisseria meningitidis* serogroup A tetrasaccharide and its conjugate. *Org. Chem. Front.* **4,** 2348–2357 CrossRef
11. Harale, K. R., Dumare, N. B., Singh, D., Misra, A. K., and Chhikara, M. K. (2015) Synthesis of a tetrasaccharide and its glycoconjugate corresponding to the capsular polysaccharide of *Neisseria meningitidis* serogroup X and its immunochemical studies. *RSC Adv.* **5,** 41332–41340 CrossRef
12. Morelli, L., Cancogni, D., Tontini, M., Nilo, A., Filippini, S., Costantino, P., Romano, M. R., Berti, F., Adamo, R., and Lay, L. (2014) Synthesis and immunological evaluation of protein conjugates of *Neisseria meningitidis* X capsular polysaccharide fragments. *Beilstein J. Org. Chem.* **10,** 2367–2376 CrossRef Medline
13. Gao, Q., Tontini, M., Brogioni, G., Nilo, A., Filippini, S., Harfouche, C., Polito, L., Romano, M. R., Costantino, P., Berti, F., Adamo, R., and Lay, L. (2013) Immunoactivity of protein conjugates of carba analogues from *Neisseria meningitidis* a capsular polysaccharide. *ACS Chem. Biol.* **8,** 2561–2567 CrossRef Medline
14. Schumann, B., Hahm, H. S., Parameswarappa, S. G., Reppe, K., Wahlbrink, A., Govindan, S., Kaplonek, P., Pirofski, L. A., Witzenrath, M., Anish, C., Pereira, C. L., and Seeberger, P. H. (2017) A semisynthetic *Streptococcus pneumoniae* serotype 8 glycoconjugate vaccine. *Sci. Transl. Med.* **9,** eaaf5347 CrossRef Medline
15. Verez-Bencomo, V., Fernández-Santana, V., Hardy, E., Toledo, M. E., Rodríguez, M. C., Heynngnezz, L., Rodriguez, A., Baly, A., Herrera, L., Izquierdo, M., Villar, A., Valdés, Y., Cosme, K., Deler, M. L., Montane, M., *et al.* (2004) A synthetic conjugate polysaccharide vaccine against *Haemophilus influenzae* type b. *Science* **305,** 522–525 CrossRef Medline
16. Fiebig, T., Romano, M. R., Oldrini, D., Adamo, R., Tontini, M., Brogioni, B., Santini, L., Berger, M., Costantino, P., Berti, F., and Gerardy-Schahn, R. (2016) An efficient cell free enzyme-based total synthesis of a meningococcal vaccine candidate. *NPJ Vaccines* **1,** 16017 CrossRef
17. Keys, T. G., Fuchs, H. L., Ehrit, J., Alves, J., Freiberger, F., and Gerardy-Schahn, R. (2014) Engineering the product profile of a polysialyltransferase. *Nat. Chem. Biol.* **10,** 437–442 CrossRef Medline
18. Romanow, A., Haselhorst, T., Stummeyer, K., Claus, H., Bethe, A., Mühlenhoff, M., Vogel, U., von Itzstein, M., and Gerardy-Schahn, R. (2013) Biochemical and biophysical characterization of the sialyl-/hexosyltransferase synthesizing the meningococcal serogroup W135 heteropolysaccharide capsule. *J. Biol. Chem.* **288,** 11718–11730 CrossRef Medline
19. Romanow, A., Keys, T. G., Stummeyer, K., Freiberger, F., Henrissat, B., and Gerardy-Schahn, R. (2014) Dissection of hexosyl- and sialyltransferase domains in the bifunctional capsule polymerases from *Neisseria meningitidis* W and Y defines a new sialyltransferase family. *J. Biol. Chem.* **289,** 33945–33957 CrossRef Medline
20. Litschko, C., Romano, M. R., Pinto, V., Claus, H., Vogel, U., Berti, F., Gerardy-Schahn, R., and Fiebig, T. (2015) The capsule polymerase CslB of *Neisseria meningitidis* serogroup L catalyzes the synthesis of a complex trimeric repeating unit comprising glycosidic and phosphodiester linkages. *J. Biol. Chem.* **290,** 24355–24366 CrossRef Medline
21. Fiebig, T., Berti, F., Freiberger, F., Pinto, V., Claus, H., Romano, M. R., Proietti, D., Brogioni, B., Stummeyer, K., Berger, M., Vogel, U., Costantino, P., and Gerardy-Schahn, R. (2014) Functional expression of the capsule polymerase of *Neisseria meningitidis* serogroup X: a new perspective for vaccine development. *Glycobiology* **24,** 150–158 CrossRef Medline
22. Fiebig, T., Freiberger, F., Pinto, V., Romano, M. R., Black, A., Litschko, C., Bethe, A., Yashunsky, D., Adamo, R., Nikolaev, A., Berti, F., and Gerardy-Schahn, R. (2014) Molecular cloning and functional characterization of components of the capsule biosynthesis complex of *Neisseria meningitidis* serogroup A: toward *in vitro* vaccine production. *J. Biol. Chem.* **289,** 19395–19407 CrossRef Medline
23. Freiberger, F., Claus, H., Günzel, A., Oltmann-Norden, I., Vionnet, J., Mühlenhoff, M., Vogel, U., Vann, W. F., Gerardy-Schahn, R., and Stum-

meyer, K. (2007) Biochemical characterization of a *Neisseria meningitidis* polysialyltransferase reveals novel functional motifs in bacterial sialyltransferases. *Mol. Microbiol.* **65,** 1258–1275 CrossRef Medline

24. Micoli, F., Romano, M. R., Tontini, M., Cappelletti, E., Gavini, M., Proietti, D., Rondini, S., Swennen, E., Santini, L., Filippini, S., Balocchi, C., Adamo, R., Pluschke, G., Norheim, G., Pollard, A., *et al.* (2013) Development of a glycoconjugate vaccine to prevent meningitis in Africa caused by meningococcal serogroup X. *Proc. Natl. Acad. Sci. U.S.A.* **110,** 19077–19082 CrossRef Medline
25. Seppälä, I., and Mäkelä, O. (1989) Antigenicity of dextran-protein conjugates in mice. Effect of molecular weight of the carbohydrate and comparison of two modes of coupling. *J. Immunol.* **143,** 1259–1264 Medline
26. Bröker, M., Dull, P. M., Rappuoli, R., and Costantino, P. (2009) Chemistry of a new investigational quadrivalent meningococcal conjugate vaccine that is immunogenic at all ages. *Vaccine* **27,** 5574–5580 CrossRef Medline
27. Forsee, W. T., Cartee, R. T., and Yother, J. (2006) Role of the carbohydrate binding site of the *Streptococcus pneumoniae* capsular polysaccharide type 3 synthase in the transition from oligosaccharide to polysaccharide synthesis. *J. Biol. Chem.* **281,** 6283–6289 CrossRef Medline
28. May, J. F., Splain, R. A., Brotschi, C., and Kiessling, L. L. (2009) A tethering mechanism for length control in a processive carbohydrate polymerization. *Proc. Natl. Acad. Sci. U.S.A.* **106,** 11851–11856 CrossRef Medline
29. Breyer, W. A., and Matthews, B. W. (2001) A structural basis for processivity. *Protein Sci.* **10,** 1699–1711 CrossRef Medline
30. Jing, W., and DeAngelis, P. L. (2004) Synchronized chemoenzymatic synthesis of monodisperse hyaluronan polymers. *J. Biol. Chem.* **279,** 42345–42349 CrossRef Medline
31. Sperisen, P., Schmid, C. D., Bucher, P., and Zilian, O. (2005) Stealth proteins: *in silico* identification of a novel protein family rendering bacterial pathogens invisible to host immune defense. *PLoS Comput. Biol.* **1,** e63 CrossRef Medline
32. DeAngelis, P. L., Oatman, L. C., and Gay, D. F. (2003) Rapid chemoenzymatic synthesis of monodisperse hyaluronan oligosaccharides with immobilized enzyme reactors. *J. Biol. Chem.* **278,** 35199–35203 CrossRef Medline
33. Xie, O., Pollard, A. J., Mueller, J. E., and Norheim, G. (2013) Emergence of serogroup X meningococcal disease in Africa: need for a vaccine. *Vaccine* **31,** 2852–2861 CrossRef Medline
34. LaForce, F. M., Konde, K., Viviani, S., and Préziosi, M.-P. (2007) The meningitis vaccine project. *Vaccine.* **25,** (Suppl. 1) A97–A100
35. Kulkarni, P. S., Socquet, M., Jadhav, S. S., Kapre, S. V., LaForce, F. M., and Poonawalla, C. S. (2015) Challenges and opportunities while developing a group A meningococcal conjugate vaccine within a product development partnership: a manufacturer's perspective from the Serum Institute of India. *Clin. Infect. Dis.* **61,** (Suppl. 5) S483–S488
36. Berti, F., Romano, M. R., Micoli, F., Pinto, V., Cappelletti, E., Gavini, M., Proietti, D., Pluschke, G., MacLennan, C. A., and Costantino, P. (2012) Relative stability of meningococcal serogroup A and X polysaccharides. *Vaccine* **30,** 6409–6415 CrossRef Medline
37. Fallarini, S., Buzzi, B., Giovarruscio, S., Polito, L., Brogioni, G., Tontini, M., Berti, F., Adamo, R., Lay, L., and Lombardi, G. (2015) A Synthetic Disaccharide Analogue from *Neisseria meningitidis* A capsular polysaccharide stimulates immune cell responses and induces immunoglobulin G (IgG) production in mice when protein-conjugated. *ACS Infect. Dis.* **1,** 487–496 CrossRef Medline
38. Berti, F., and Adamo, R. (2013) Recent mechanistic insights on glycoconjugate vaccines and future perspectives. *ACS Chem. Biol.* **8,** 1653–1663 CrossRef Medline
39. Avci, F. Y., Li, X., Tsuji, M., and Kasper, D. L. (2011) A mechanism for glycoconjugate vaccine activation of the adaptive immune system and its implications for vaccine design. *Nat. Med.* **17,** 1602–1609 CrossRef Medline
40. Vionnet, J., and Vann, W. F. (2007) Successive glycosyltransfer of sialic acid by *Escherichia coli* K92 polysialyltransferase in elongation of oligosialic acceptors. *Glycobiology.* **17,** 735–743 CrossRef Medline
41. Linding, R., Russell, R. B., Neduva, V., and Gibson, T. J. (2003) GlobPlot: exploring protein sequences for globularity and disorder. *Nucleic Acids Res.* **31,** 3701–3708 CrossRef Medline
42. Kelley, L. A., Mezulis, S., Yates, C. M., Wass, M. N., and Sternberg, M. J. (2015) The Phyre2 web portal for protein modeling, prediction and analysis. *Nat. Protoc.* **10,** 845–858 CrossRef Medline
43. Kavoosi, M., Creagh, A. L., Kilburn, D. G., and Haynes, C. A. (1996) Strategy for selecting and characterizing linker peptides for CBM9-tagged fusion proteins expressed in *Escherichia coli*. *Biotechnol. Bioeng.* **98,** 599–610 Medline